# DCL-SLAM: A Distributed Collaborative LiDAR SLAM Framework for a Robotic Swarm

Shipeng Zhong, Yuhua Qi\*, Zhiqiang Chen, Jin Wu, Hongbo Chen, and Ming Liu

Abstract-To execute collaborative tasks in unknown environments, a robotic swarm must establish a global reference frame and locate itself in a shared understanding of the environment. However, it faces many challenges in real-world scenarios, such as the prior information about the environment being absent and poor communication among the team members. This work presents DCL-SLAM, a fully distributed collaborative LiDAR SLAM framework to co-localize simultaneously in an unknown environment with minimal information exchange. Based on peer-to-peer communication (limited bandwidth and communication range), DCL-SLAM adopts the lightweight LiDAR-Iris descriptor for place recognition and does not require full connectivity among teams. DCL-SLAM includes three main parts: a replaceable single-robot front-end LiDAR odometry; a distributed loop closure module that detects overlaps between robots; and a distributed back-end module that adapts distributed pose graph optimizer combined with rejecting spurious loop measurements. We integrate the proposed framework with diverse open-source LiDAR odometry to show its versatility. The proposed system is extensively evaluated on benchmarking datasets and field experiments over various scales and environments. Experimental result shows that DCL-SLAM achieves higher accuracy and lower communication bandwidth than other state-of-art multi-robot SLAM systems. The source code and video demonstration are available at https://github.com/PengYu-Team/DCL-SLAM.

## I. INTRODUCTION

Simultaneous Localization and Mapping (SLAM) is a fundamental capability in robot navigation, especially in unknown and GPS-denied environments, and there is a substantial body of literature dedicated to advanced single-robot SLAM methods [1], [2], [3]. However, compared to a single-robot system, the multi-robot system has a more remarkable ability and work efficiency in time-sensitive applications such as factory automation, exploration of unsafe areas, intelligent transportation, and search-and-rescue in military and civilian endeavors. Hence, various collaborative SLAM methods (C-SLAM) for robotic swarms have been studied in the last decade based on single-robot SLAM [4]. C-SLAM aims to combine data from each robot and establish relative pose transformations and a global map between robots.

For the real-world application of robotic swarms, however, C-SLAM remains an open problem and faces several challenges currently being researched since communication among the robots may be slow (bandwidth constraints) or infeasible (limited communication range). Due to the various

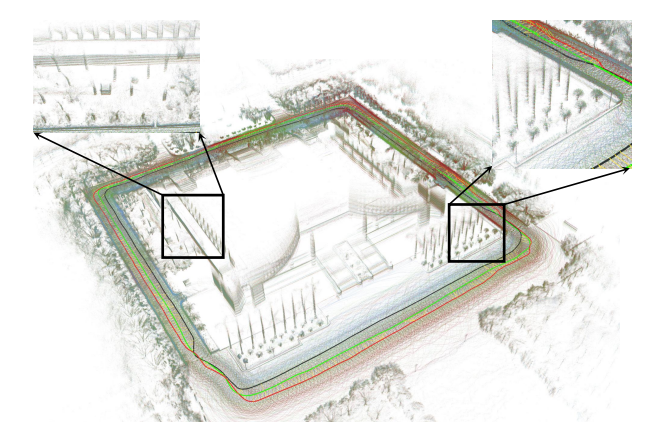


Fig. 1. The reconstructed maps and trajectories derived by DCL-SLAM framework with three robots, shown in green, red and blue, at Sun Yat-Sen University's eastern campus library.

advantages of LiDAR, such as high-resolution point cloud and robustness to a wide range of weather and lighting conditions, many LiDAR C-SLAM methods have been proposed, e.g., LAMP [5], LAMP 2.0 [6], SegMap [7], DiSCo-SLAM [8]. In works [5], [6], the local maps produced by each robot were directly transmitted to a server for centralized optimization, which requires higher computation and communication performance. To reduce bandwidth consumption, SegMap [7] proposed a data-driven descriptor for 3D LiDAR. However, it is still a highly centralized system and difficult to be applied in a large-scale robotic swarm. DiSCo-SLAM [8] firstly exchanges lightweight LiDAR features in a distributed manner, but it does not apply in online and field experiments with multi-robots. In addition, many C-SLAM works [7], [8] evaluate their system by splitting a whole dataset into multiple parts, which cannot represent the actual cooperation of robotic swarms. Therefore, gathering synthetic data from multiple platforms in real scenarios for system evaluation is necessary. C-SLAM is still a relatively young research field in the research community, albeit very promising.

In this spirit, we present DCL-SLAM, a fully-distributed collaborative LiDAR SLAM framework for robotic swarms. DCL-SLAM focuses on data-efficient and resilient interrobot communication, reaching a consistent trajectory estimate with partial pose measurements and indirect data association. Our framework is compatible with various LiDAR odometry users prefer with absolutely no additional effort. When there is no teammate within communication range, each robot performs single-robot front-end independence to ensure the autonomy of each robot. To satisfy the communication constraints, a lightweight global LiDAR descriptor, LiDAR-Iris [9], is integrated to describe LiDAR scans and

S. Zhong, Y. Qi, Z. Chen and H. Chen are with School of Systems Science and Engineering, Sun Yat-Sen University, China (Corresponding Author: Yuhua Qi, Email:qiyh8@mail.sysu.edu.cn)

J. Wu and M. Liu are with Department of Electronic and Computer Engineering, Hong Kong University of Science and Technology, Hong Kong, China. e-mail: eelium@ust.hk

detect loop closures without exchanging extra raw data. To avoid double counting, we design a three-stage inter-robot loop closure detection approach to obtain relative pose transformations between robots. First, as descriptors are received from other robots, the recipient robot finds inter-loop closure candidates and sends filtered LiDAR scans back. Next, the sender robot performs a geometry verification and calculates a shared relative pose transformation for the recipient robot. After that, outlier rejection based on [10] is performed to remove spurious inter-robot loop closures for robustness. Finally, all collected measurements are optimized together by a two-stage distributed Gauss-Seidel (DGS) approach [11], which requires minimal information exchange. Our framework is evaluated using several multi-robot datasets, including public datasets (KITTI) and a unique dataset gathered with three unmanned ground vehicles (UGVs). Furthermore, online field experiments are also presented.

To summarize, the contributions of this work are the following:

- A fully-distributed collaborative LiDAR SLAM framework for the robotic swarm (here UGVs, equipped with a 3D LiDAR and an IMU) is presented. It is adaptable to different LiDAR front-end and enables distributed state estimation at the back-end, ensuring the independence of each robot.
- A highly-integrated data-efficient inter-robot loop closure detection approach is proposed to achieve high accuracy and robustness by adapting a global LiDAR descriptor for place recognition.
- Experimental evaluation of DCL-SLAM, including benchmarking datasets and real-world field tests on campus, is presented. We also demonstrate many integrated results with various LiDAR front-end methods to verify the versatility of the proposed framework.
- The source code of the proposed system is open to the public with ease-to-run demonstrations.

The rest of this paper is organized as follows. After reviewing the relevant C-SLAM and place recognition background literature in Section II, a framework for the proposed DCL-SLAM is presented in Section III. Experimental results are given in Section IV, with conclusions in Section V.

#### II. RELATED WORK

Collaborative SLAM. The literature on C-SLAM systems distinguishes between centralized and distributed architectures. Centralized approaches collect all measurements at a central station (or robot) and estimate the trajectory for all the robots. The centralized C-SLAM in related work investigates different sensing modalities, including laser [12], [7], [5] and vision [13], [14], [15]. Dube et al. [12] segmented the local laser maps and collected all segments to detect loop closure. SegMap [7] introduced a lightweight descriptor for laser point cloud to extract meaningful features that can also be used for loop detection and map reconstruction in the server. LAMP [5] achieved a common frame by detecting artifacts with YOLO. CVI-SLAM [14], CCM-SLAM [13], and COVINS [15] offloaded the local visual odometry keyframes

to a server, used a bag-of-words approach to find overlaps and optimized with global BA.

Still, distributed SLAM [8], [16], [17], [18], [19], [20], [21] is more suitable for a multi-robot system under poor communication due to the bandwidth constraints and limited communication range. DDF-SAM [16] proposed a distributed trajectory optimization method based on Gaussian elimination, transmitting the Gaussian edge variable for place recognition. Choudhary et al.[18] proposed a two-stage distributed Gauss-Seidel method and evaluated it in objectbased SLAM. Literature [17] performed efficient data association for inter-loop closure in two stages in a distributed manner with NetVLAD. Based on [18], DOOR-SLAM [20] detected inter-robot loop closures with lightweight NetVLAD descriptors, and used pairwise consistent measurement set maximization algorithm to reject spurious loop closures. SLAMM [19], an extension to ORB-SLAM, added a fourth thread to handle the multiple maps generated by running numerous robots. Kimera-Multi [21] used the bag-of-words approach for distributed place recognition and adopted a robust pose graph optimization with incremental maximum clique outlier rejection. The most similar work to our method is DiSCo-SLAM [8], which proposed a two-stage local and global distributed optimization framework and introduced lightweight LiDAR features for loop closure. Our method is different in two aspects: First, considering bandwidth limitation and communication range, we proposed a distributed loop closure detection framework without exchanging raw sensing data. Second, we apply our system in online field tests with three robots when DiSCo-SLAM runs only in a dataset collected by one robot.

Place recognition. Generally, place recognition methods on the 3D point cloud can be divided into local descriptors, global descriptors, and learning-based approaches. Local descriptor was extracted from the local neighborhood of the keypoint in the point cloud. However, local descriptors methods are unsuitable for C-SLAM scenarios due to the lack of descriptive power. Extracting global descriptors from entire set of point can mitigate this problem, such as GRSD [22], M2DP [23], Scan-Context[24], DELIGHT [25] and LiDAR-Iris [9]. M2DP projected points onto multiple planes, and the histogram of point count in each bin on each projection plane was concatenated to get a signature of the point cloud. DELIGHT divided the scan sphere into 16 parts, and each part's histogram of LiDAR intensity was concatenated to represent the point cloud. Scan-Context exploited the expanded bird-eye view of the point cloud and represented it by the histogram of the maximal height of each bin on the horizontal plane. Recently, convolutional neural networks have been used to train feature descriptors [7]. However, these learning-based approaches require tremendous amounts of training data. In our work, we adopted LiDAR-Iris for fast and robust place recognition. LiDAR-Iris is similar to Scan Context, but it encodes height information of each bin, extracts discriminative features without any pre-training, and is rotation-invariant without brute-force matching.

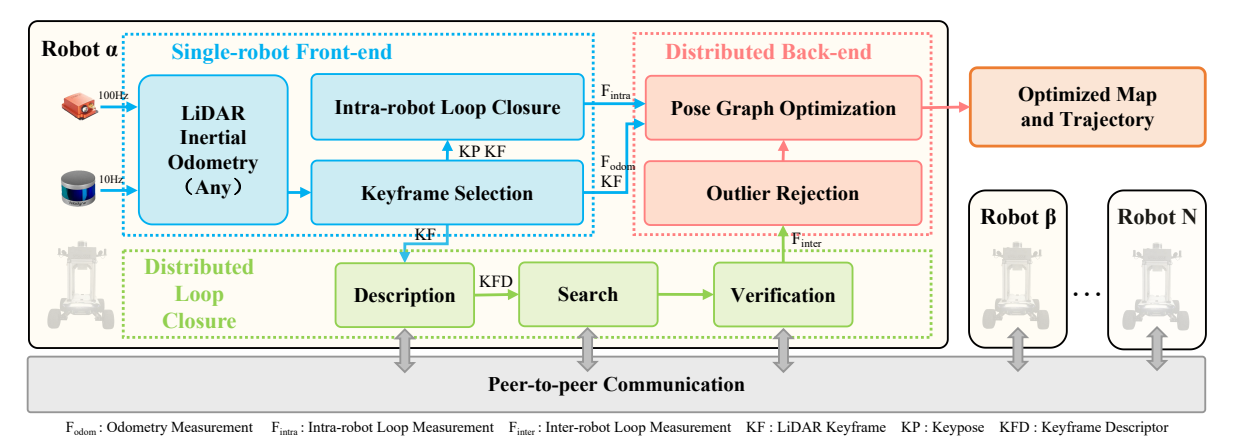


Fig. 2. The proposed fully-distributed collaborative LiDAR SLAM, DCL-SLAM, consists of a replaceable single-robot front-end module to produce odometry factor and intra-robot loop factor, a distributed loop closure module for detecting inter-robot loop closures, a distributed pose graph optimization module to estimate the global trajectories for the robotic swarm combined with rejecting spurious loop measurements, and a peer-to-peer communication module to exchange necessary data (descriptors, measurements, pose estimates, etc.).

#### III. THE DCL-SLAM FRAMEWORK

Our proposed framework relies on peer-to-peer communication with the ad-hoc wireless network. When two robots rendezvous, they share the understanding of the environment information to establish a global reference frame and perform distributed SLAM. Moreover, each robot performs single-robot SLAM when there is no teammate within the communication range to ensure the independence of each robot.

In some existing C-SLAM systems [7], the front-end and back-end modules are tightly entangled, making it difficult to replace or update one improved module (e.g., odometry, inter-robot loop closure) at a low-cost. Therefore, our framework is modularized into three main parts: a single-robot front-end, distributed loop closure, and distributed back-end. An overview of our proposed DCL-SLAM framework is given in Fig. 2. Each robot collects raw data from a LiDAR and an inertial measurement unit (IMU) and locally runs a single-robot front-end module (Section III-A) to produce an estimate of its trajectory. In distributed loop closure module (Section III-B), a keyframe scan is selected from odometry pose and then described as a global descriptor (LiDAR-Iris [9]) for performing place recognition among the robots. Each robot communicates to other robots within the communication range with the descriptor for performing inter-robot loop closure detection. The output loop closure candidates are then verified using either the raw point cloud or the features point cloud with ICP and random sample consensus (RANSAC) to get inter-robot loop closure measurements. After that, the distributed back-end module module (Section III-C) module collects all odometry measurements, intrarobot loop measurements, and inter-robot loop measurements to compute the maximal set of pairwise consistent measurements (PCM) [10] and filters out the outliers. The optimal trajectory estimation of the robotic swarm is solved using a two-stage distributed Gauss-Seidel method proposed in [18] for reaching an agreement on the pose graph configuration.

## A. Single-robot Front-end

The DCL-SLAM framework support interface with single-robot front-ends with various LiDAR odometry and is com-

patible with different LiDAR configurations (e.g., solid-state LiDAR and mechanical LiDAR). In our implementation, LIO-SAM [2], FAST-LIO2 [3] are adopt as our single-robot front-end, and other LiDAR odometry such as LOAM [26] and LiLi-OM [27] are an alternative. Once the odometry estimate is refined, the LiDAR odometry factor  $F^i_{odom}$  ( $i \in \{\alpha, \beta, \gamma, \cdots\}$ ) can be constructed and sent to the distributed back-end module. The correlative point cloud scan  $S^i$  is used for intra-robot and inter-robot loop closure.

To improve the accuracy of the single-robot front-end module, an intra-robot loop closure submodule to eliminate the odometry drift is necessary. In some existing LiDAR odometry (e.g., LIO-SAM), the intra-loop closure submodule is included. Therefore, it is easy to extract the results to construct the intra-robot loop closure factor  $F^i_{intra}$  for the pose distributed graph optimization. In addition, we also provide a built-in intra-robot loop closure submodule in our framework for only odometry systems (e.g., FAST-LIO2), familiar with the inter-robot loop closure module without communication with other robots (see details in the following subsection).

## B. Distributed Loop Closure

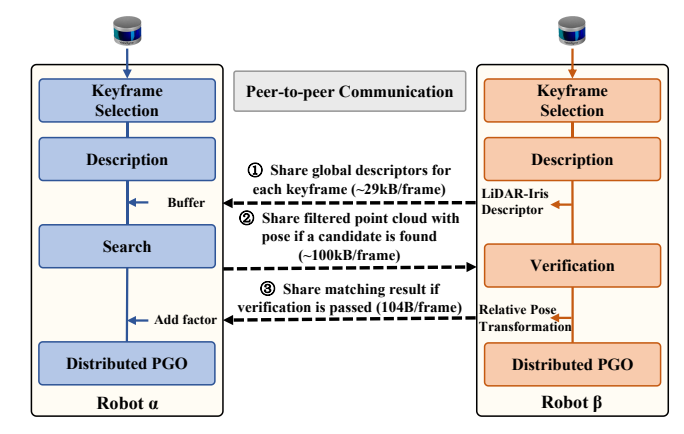


Fig. 3. Illustration of the distributed loop closure module from robot  $\alpha$ 's perspective (using VLP-16).

In our framework, the distributed loop closure module performs place recognition among robotic swarms to generate the relative poses transformation and is illustrated in Fig. 3. Moreover, it is a crucial module to detect overlap parts between local maps created by itself or other robots in the swarm to reduce its accumulated drift or fuse all robots into a geometrically consistent global map. Our distributed loop closure module consists of four steps: keyframe selection, description, search, and verification. To improve the computation and communication efficiency, we first select keyframes depending on the movement change. Furthermore, we perform a three-stage distributed loop closure detection approach, including sharing global descriptors for each keyframe, sharing filtered point cloud with pose if a candidate is found, and sharing matching result if verification pass. It can permit data-efficient communication and does not require full connectivity among the robotic swarm. An overview of communication consumption in the field test is given in Section IV.

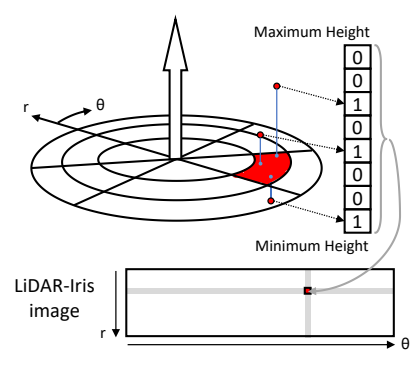


Fig. 4. Demonstration of encoding the LiDAR scan into the LiDAR-Iris descriptor.

**Description**. Many global or local descriptor matching suffers from the lack of descriptive power or the struggle with invariance, which would be problematic in a robotic swarms scenario. For this reason, we rely on LiDAR-Iris[9], a state-of-the-art global LiDAR descriptor for place recognition that is rotation-invariant without brute-force matching and robust to sparse and inconsistent point clouds. As shown in Fig. 4, LiDAR-Iris projects LiDAR point cloud to its bird-eye view and divides into  $N_r$  (radial direction)  $\times N_a$  (angular direction) bins according to the angular and radial resolution:

$$I = (a_{ij}) \in \mathbb{R}^{N_r \times N_a}. \tag{1}$$

Each bin encodes height information into an 8-bit binary code as the pixel intensity of the LiDAR-Iris image. Four 1D LoG-Gabor filters are exploited to convolve each row of the LiDAR-Iris image to enhance the representation ability. A discriminative binary feature map is obtained by applying a simple thresholding operation on convolutional responses. This description procedure does not require counting the points in each bin and pre-train model.

In this paper, for Velodyne HDL-64E (KITTI dataset) and VLP-16 (our dataset),  $N_r$  is 80 and  $N_a$  is 360. In each robot, the LiDAR scan generated by LiDAR odometry will firstly be downsampled by a voxel filter. Then the filtered scan will be locally described as a binary feature map with a LiDAR-Iris image. As shown in Fig. 3, once robot  $\beta$  is in the communication range of robot  $\alpha$ , the binary feature maps

of robot  $\beta$  are sent to robot  $\alpha$  alone with row keys (about 29kB per keyframe). Therefore, robot  $\alpha$  can obtain a history database of LiDAR-Iris binary features for all robots.

**Search**. The recipient robot (robot  $\alpha$ ) searches for neighbors of the shared LiDAR-Iris descriptor in its respective KD-tree. For fast searching and rotation invariance, each robot further reduces the LiDAR-Iris image to a  $N_r \times$  one vector as query row key by encoding each image row into a single value via a  $L_2$  norm. In the search stage, a row key KD-tree is built for loop closure candidate search. To deal with the viewpoint changes of LiDAR (e.g., revisit in the opposite direction), a Fourier transform is adopted to estimate the translation between two LiDAR-Iris images, making it rotation-invariant concerning odometry pose. The top N-matched query key's binary feature maps are compared against the query binary feature map using Hamming distance. The closest candidate to the query satisfying an acceptance threshold is regarded as a loop-closure candidate and shared with robot  $\beta$ :

$$d = \sum_{r=1}^{N_r} \sum_{ij}^{N_a} b_{ij}^{\alpha} \oplus b_{ij}^{\beta}, \tag{2}$$

where  $b_{ij}^{\alpha}$  is the binary feature of  $a_{ij}^{\alpha} \in I^{\alpha}$  and  $\oplus$  is XOR operation. Robot  $\alpha$  also transmitted the filtered features cloud or filtered deskewed cloud of the recognized place to robot  $\beta$  for verification (about 100kB per frame). This stage provides a loop closure candidate without exchanging the raw data and does not require full connectivity.

**Verification**. In the verification stage, the candidate matching items are then verified by a scan-to-map matching performed on the filtered scan of robot  $\alpha$  and the surrounding submap of robot  $\beta$  using RANSAC. If the set of inliers is sufficiently large, it considers the corresponding loop closure successful. The relative pose transformation of the loop closure candidate is evaluated using ICP. After that, robot  $\beta$  feeds back the relative pose transformation of the interrobot loop closure to robot  $\beta$  (about 104B per keyframe). Once the inter-robot loop factor  $F_{inter}^i$  is found and shared, both robots initiate the distributed pose graph optimization described in the following section.

## C. Distributed Back-end

In our DCL-SLAM framework, the distributed back-end module includes two submodules. The first submodule, outlier rejection, removes spurious inter-robot loop closures. The second submodule, pose graph optimization (PGO), constructs a global pose graph with three types of factors (odometry factor, intra-robot, and inter-robot loop factor) to estimate the global trajectories for the robotic swarm.

**Outlier Rejection**. The distributed outlier rejection submodule rejects false-positive inter-robot loop closures caused by only matching features in the loop finding procedure. These perceptual aliasing may cause a considerable drift in the robot trajectory estimation. Therefore, pairwise consistent measurements set maximization in [10] is introduced for outlier rejection and implemented as distributed and incremental approach. PCM checks the consistency of pairs of inter-robot

loop closures  $z_{\alpha_i\beta_m}$  and  $z_{\alpha_i\beta_n}$  by the following metric:

$$||(z_{\alpha_i\alpha_j} \cdot z_{\alpha_j\beta_m} \cdot z_{\beta_m\beta_n}) \cdot z_{\alpha_i\beta_n}^{-1}||_2^2 < \varepsilon, \tag{3}$$

where  $z_{\alpha_i\alpha_j}$  is a intra-robot pose transformation related to time i and j in robot  $\alpha_i$ ,  $z_{\alpha_j\beta_m}$  is a inter-robot pose transformation related to time j in robot  $\alpha$  and m in robot  $\beta$ , and  $\varepsilon$  is the likelihood threshold. After the pairwise consistency checks are performed, it finds the largest set of pairwise consistent measurements by finding a maximum clique. Finally, the loop closures in the set are passed to back-end distributed PGO.

**Pose Graph Optimization**. The PGO submodule uses the odometry measurements and the loop closures measurements (intra-robot and inter-robot) to estimate the trajectories of the robots by solving a maximum likelihood problem:

$$x^* = \arg\max_{x} \prod \psi(z_{\alpha_i}^{\beta_m} \mid x), \tag{4}$$

where  $x = [x_{\alpha}, x_{\beta}, ...]$  is a set of poses of all robot trajectories,  $\psi(\cdot)$  is a likelihood item,  $z_{\alpha_i}^{\beta_m}$  is a general measurement model. In our implementation, the distributed PGO method in [11] is adopted, which solves distributed pose graph optimization using a distributed two-stage Gauss-Seidel method. It first estimates the rotations of the trajectories of the robots and then estimates the full pose with the optimized rotations. With this approach, the robots in the swarm can exchange minimal information to avoid complex bookkeeping and double counting and reach a consensus on the optimal trajectory estimate.

## IV. EXPERIMENT

This section showcases the performance, accuracy, and communication of DCL-SLAM evaluated in several scenarios and provides experimental results compared to other state-of-art C-SLAM and single-robot systems.

## A. Experimental Setup

1) Single-robot SLAM and C-SLAM systems: The proposed DCL-SLAM system results from the combination of many frameworks and libraries. The system uses the robot operating system (ROS) to interface with the attached sensors and handles information of different modules exchanged between robots. All methods are implemented in C++ and executed using ROS in Ubuntu 18.04 LTS. To show the extensibility of our framework, we integrate existing open-source LiDAR odometry methods with DCL-SLAM and release the code for ease of use, including LIO-SAM<sup>1</sup> and FAST-LIO2<sup>2</sup>. Moreover, we adopt the C++ implementation of LiDAR-Iris provided in [9] with default parameters (the descriptor size is  $80\times360$ ) and exchange descriptors among the robotic team. Furthermore, the inter-loop closure candidates are found by searching the row key of the descriptor with the k-nearest neighbor algorithm implemented in the libnabo library. As for back-end optimization, we refer to distributed estimation method in [11] to implement the distributed PGO module using the GTSAM library.

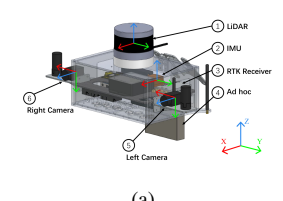




Fig. 5. (a) The sensor configuration for our own datasets collected at Sun Yat-Sen University's eastern campus. Note that the attached camera doesn't use in the following test scenes. (b) Robotic swarm of Agilex SCOUT MINI.

2) Hardware Setup: As shown in Fig. 5(a), the UGVs used in our tests are Agilex SCOUT MINI, equipped with a Velodyne VLP-16 Puck LiDAR, an Xsens MTi-30 IMU, and an onboard computer NUC11PAKi7 (Intel i7-1165G7 CPU, 16GB DDR4 RAM). The LiDAR is configured to have a 10 Hz update rate and IMU updates at 100 Hz. The UGV relies on communication radio NexFi MF1400 which creates an adhoc wireless network to provide peer-to-peer communication between robots.

 $\label{eq:TABLE} \textbf{TABLE I}$  Details of Public and Our Collected Datasets

	Datasets	Environment	Trajectory Length [m]					
Datasets		Environment	Robot $\alpha$	Robot $\beta$	Robot $\gamma$			
	Seq. 05	urban	424.9	599.9	1066.7			
KITTI	Seq. 08	urban	1252.8	1991.6	-			
×	Seq. 09	urban	557.4	733.2	544.4			
SYSU's Campus	Square_1	campus	455.6	454.4	458.2			
	Square_2	campus	250.6	246.4	-			
	Library	campus	507.6	517.2	498.9			
	Playground	campus	407.7	425.6	445.5			
	Dormitory	campus	727.0	719.3	721.9			
	College	campus	920.5	995.9	1072.3			
<b>J</b> 1	Teaching_Building	indoor	617.2	734.4	643.4			

3) Datasets: All experimental results in this paper are obtained by comparing performance on three KITTI odometry sequences (HDL-64) and seven collected on SYSU's eastern campus (VLP-16). For KITTI odometry sequences, we especially adopt the sequences 05, 08, and 09 among 11 sequences, as they have a variety of loop closure types, including the same and opposite viewpoints. Furthermore, we split sequences 05 and 09 into three parts and sequence 08 into two to simulate multi-robot scenarios. The sequences from KITTI provide GNSS ground-truth data for experimental evaluation. In addition, six outdoor sequences and one indoor are collected with a robotic swarm in different scenarios at Sun Yat-Sen University's eastern campus, as shown in Fig. 5(b). The indoor sequence is an online experiment specifically for outliers rejection. Real-time kinematic (RTK) provide the ground-truth data in the outdoor sequences. Table I recaps the main characteristics for all sequences used in experiments. We used the evo [28] tool to evaluate and compare the trajectory output of odometry and C-SLAM

<sup>&</sup>lt;sup>1</sup>https://github.com/PengYu-Team/DCL-LIO-SAM

<sup>&</sup>lt;sup>2</sup>https://github.com/PengYu-Team/DCL-FAST-LIO

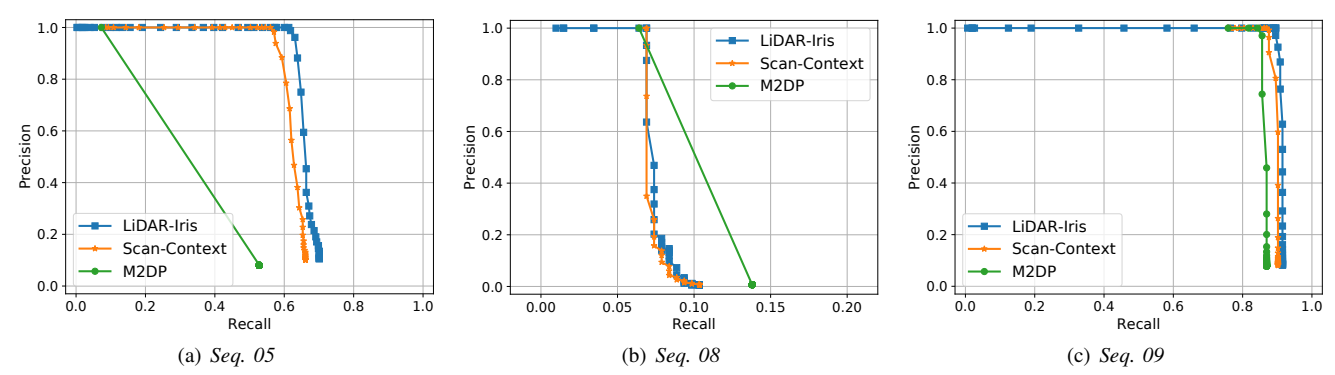


Fig. 6. The precision-recall curves of different methods on different KITTI sequences.

algorithms for KITTI and our outdoor sequences.

## B. Performance of Distributed Loop Closure

To obtain the true-positive and recall rate and further the best threshold of matching distance, we used the original laser scan from the KITTI sequences to compare the performance of all descriptor methods and assumed that all robots start simultaneously. The closest candidate produced by matching the history database is regarded as an interrobot loop closure candidate and further verified against the ground truth. If the ground truth distance between the current query and the closest match is less than 4m, the candidate is regarded as a true positive. Note that the 4m-distance is set as default according to [24], and default parameters are set for LiDAR-Iris, Scan-Context, and M2DP.

As shown in Fig. 6, M2DP only reported high precision with a lower recall rate, which shows that M2DP can detect the simple inter-loops correctly. Compared to M2DP, Scan-Context can achieve promising results on all three sequences. In contrast, LiDAR-Iris demonstrates very competitive performance on all three sequences and achieves the best performance on *Seq. 05* and *Seq. 09*, which shows its advanced performance in detecting various inter-loops. Regarding computational complexity, the average matching time of LiDAR-Iris on *Seq. 08* is 24.57ns, the time of Scan-Context is 6.71ns, and the time of M2DP is 0.01ns.

## C. System Evaluation

To evaluate the accuracy and the robustness of the whole SLAM system, we compared the proposed method to DiSCo-SLAM and single-robot SLAM systems on KITTI odometry datasets, and the result ATE and ARE are shown in Tab. II. In addition, Fig. 7(a)-(e) present the trajectories result of different method on *Seq. 05*. As illustrated in the table, the performance of DCL-SLAM with different odometry, including LIO-SAM (named DCL-LIO-SAM) and FAST-LIO2 (named DCL-FAST-LIO2), is always better than that of only odometry (). The reason is that DCL-SLAM introduces more measurements between robots for back-end optimization. The table also shows us that DCL-SLAM successfully merges the sub-maps in *Seq. 05* and *Seq. 09* when DiSCo-SLAM failed. Moreover, our DCL-SLAM has a smaller ATE, but a larger ARE than DiSCo-SLAM on *Seq. 08*, and reach

TABLE II
ESTIMATION ACCURACY OF THE KITTI ODOMETRY SEQUENCES

Seq.	Configure	A	TE [m	n]	ARE [deg]			
Scq.	Configure	Robot $\alpha$	Robot $\beta$	Robot $\gamma$	Robot $\alpha$	Robot $\beta$	Robot $\gamma$	
	DiSCo-SLAM		Failed		Failed			
	only LIO-SAM	1.04	1.70	0.90	1.50	2.82	2.28	
Seq. 09	our DCL-LIO-SAM	1.07	1.40	0.85	1.46	2.64	2.20	
	only FAST-LIO2	1.08	4.14	0.77	2.91	15.51	1.97	
	our DCL-FAST-LIO2	0.95	2.46	0.70	2.83	8.77	1.73	
	DiSCo-SLAM	5.16	5.73	-	6.12	5.47	-	
	only LIO-SAM	5.57	5.53	-	6.46	5.71	-	
Seq. 08	our DCL-LIO-SAM	4.92	4.87	-	6.25	5.69	-	
	only FAST-LIO2	5.29	4.98	-	5.58	6.25	-	
	our DCL-FAST-LIO2	4.58	4.54	-	5.15	6.04	-	
	DiSCo-SLAM	Failed			Failed			
	only LIO-SAM	0.30	1.21	2.80	1.47	1.48	11.34	
Seq. 05	our DCL-LIO-SAM	0.25	0.44	1.08	1.43	1.14	1.12	
	only FAST-LIO2	0.46	0.90	2.30	2.51	2.25	2.25	
	our DCL-FAST-LIO2	0.55	1.05	1.34	1.93	2.00	1.82	

the best in Seq. 05 and Seq. 09. These illustrate that DCL-SLAM has higher precision and good robustness.

In order to further evaluate the accuracy and robustness of the proposed system and overcome the reality gap, we deployed UGVs on our campus for field tests and recorded datasets, as shown in section IV-A. Similar to the above public datasets evaluation, we compared the proposed DCL-SLAM to DiSCo-SLAM and single-robot SLAM systems on recorded campus datasets. The ATE result is shown in Tab III. Furthermore, the results of the trajectories and reconstructed maps of the UGVs on sequence Library performed by DLC-LIO-SAM are presented in Fig. 1. In addition, Fig. 7(f)-(j) present the trajectories output of different method on sequence *College*. These results show that DiSCo-SLAM behaved well in some sequences but failed to merge all or part of the sub-maps in most sequences. As opposed to DiSCo-SLAM, our DCL-LIO-SAM approach demonstrates very competitive performance on most sequences and reaches the best on Square\_1, Library, Dormitory and College sequences. Compared to using odometry only, DCL-SLAM reported similar performance on two Square sequences because the system can only merge the sub-maps with simple inter-loops, leaving the challenging ones. Moreover, DCL-SLAM improves performance by over 20% on the other four sequences. Note that FAST-LIO has degradation of the

TABLE III
ATE W.R.T RTK OF THE SYSU'S EASTERN CAMPUS DATASETS

	Datasets		Square_	1	Squa	ire_2		Library		P	laygroui	ıd	I	Oormitor	у		College	
Configure		Robot α	Robot $\beta$	Robot $\gamma$	Robot α	Robot $\beta$	Robot α	Robot $\beta$	Robot $\gamma$	Robot α	Robot $\beta$	Robot $\gamma$	Robot α	Robot $\beta$	Robot $\gamma$	Robot α	Robot $\beta$	Robot $\gamma$
DiSCo-	SLAM		Failed		Fai	led	0.74	1.33	1.27	0.27	0.37	0.38		Failed			Failed	
only LIC	O-SAM	1.23	0.92	0.69	0.46	0.27	1.03	1.74	1.30	0.35	0.72	0.45	0.82	1.71	0.70	2.35	4.58	1.41
our DCL-I		1.23	0.86	0.66	0.50	0.26	0.58	1.26	1.17	0.33	0.40	0.32	0.52	1.37	0.51	1.51	1.48	1.87
only FAS		1.58	2.87	0.72	1.47	0.60	1.53	2.29	1.10	0.48	0.76	0.77	9.30	6.28	2.39	3.63	5.69	12.88
our DCL-F.	AST-LIO2	1.56	2.87	0.72	1.45	0.60	1.30	1.38	1.07	0.58	0.68	0.40	6.91	5.64	2.33	6.13	3.27	3.30
### Grand Truth ####################################	100 x (m)	200	200 200 -100 -200	3 -100 x	( = n	abot p	400 Ground Robots 300 Robots -	α β γ γ	0 100 m)	200	300	-100 x 6	R R R R	round Trush about a sale a sal	300		=	Ground Truth Robot a Robot β Robot y
(a) L	JO-SAM		(t	) FAST	LIO2		(c)	DiSCo	-SLAM		(d)	DCL-L	IO-SAN	1	(e)	DCL-FA	AST-LIC	02
100 0 0 0 0 0 0 0 0 0 0 0 0 0 0 0 0 0 0		round Truth door or door y	100 0 0 -200 -300 -200 -1	00 0 100 x	- A	round Truth book a book of boo	100 Ground Robbel Robbel Robbel 200 -1	is a series of the series of t	200 300 m)	400	100 - Ground Redon	12 (A)	(m) 200 300	460	100 - Group Robe Robe Robe Robe Robe - Robe	ot α	0 200 300	400
(f) L	IO-SAM		(g	g) FAST	LIO2		(h)	DiSCo	-SLAM		(i)	DCL-LI	O-SAM	I	(j) ]	DCL-FA	ST-LIO	2

Fig. 7. The trajectories result over the KITTI Seq. 05 (from (a) to (e)) and our College (from (f) to (j)), with different method. Note that the trajectories of LIO-SAM and FAST-LIO2 are the results of a single robot starting from inertial frame, which are not aligned to the ground true.

LiDAR odometry accuracy of the z-axis on *Dormitory* and *College* sequences, leading to the larger ATE of trajectory compared to the RTK ground true. In this case, DLC-FAST-LIO2 cannot properly correct the odometry's drift. In general, DCL-SLAM has high precision and broad applicability.

## D. Field Test with Outlier Rejection

We also experimented in a teaching building on our campus, an environment with severe perceptual aliasing, with a PCM threshold of 5.348 and an inlier threshold of 0.3 for geometric verification using RANSAC. Fig. 8 reports the trajectories and mapping results of DCL-LIO-SAM with and without the PCM approach. The output trajectories of the robotic swarm with the PCM method in Fig. 8(b) are more consistent with the surrounding environment than that in Fig. 8(a), which explains the necessity of introducing an outlier rejection module.

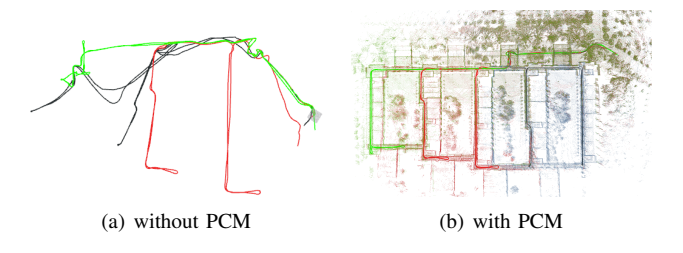


Fig. 8. The trajectories result of DCL-LIO-SAM on *Teaching\_building* sequence, where robot  $\alpha/\beta/\gamma$  is represented by green/red/blue.

TABLE IV

NETWORK TRAFFIC OF EACH AGENT AVERAGED OVER SEQUENCES

	Datasets	Avg. Tra	ansmit Dat Robot β	a [kB/s] Robot γ	Communication Time [s]
	Seq. 09	92.93	177.30	91.14	101.24
H	Seq. 08	161.78	160.93	-	191.86
KITT	Seq. 05	81.08	143.41	187.73	251.70
	Avg. (3 Seq.)		164.67		181.60
	Library	34.43	60.51	43.92	1014.44
Campus	College	66.98	67.48	57.98	1188.84
	Square_1	41.75	40.68	37.89	538.99
	Avg. (3 Seq.)		53.55		914.09

## E. Communication

To quantify the bandwidth requirements of the proposed DCL-SLAM system, we also counted the network traffic on public (HDL-64) and our campus datasets (VLP-16), and the mean bandwidth is shown in Tab. IV. Note that we assume there are no communication range constraints in the robotic swarm so that messages can be exchanged at any time. For *Library* sequence, the distributed PGO requires the transmission of 3.46 MB, while the centralized one requires 10.06 MB to transmit the whole pose graph.

Furthermore, we counted the sizes of messages sent among swarm on our datasets, as shown in Tab. V. In DCL-SLAM, the transmitted data can be broadly grouped into keyframe, inter-robot match, and distributed PGO. Firstly, the keyframe message in DCL-SLAM is extracted from the keyframe 3D point cloud. While a single laser scan from

TABLE V
Data Size of Messages Sent (VLP-16)

Informati	Avg.Size [kB] $\pm$ Std.	
Keyframe	LiDAR-Iris Descriptor Feature Cloud*	$\begin{array}{c} 29.12\pm0.00 \\ 160.24\pm16.00 \end{array}$
Inter-robot Match	Loop Closure Measurement Verification Point Cloud Raw Point Cloud*	$0.11 \pm 0.00$ $99.92 \pm 13.96$ $384.76 \pm 30.76$
Distributed PGO	Pose Estimate	$0.10\pm0.00$

<sup>\*</sup> The messages sent in case the robots were to directly transmit raw data.

VLP-16 is 1 MB and from HDL-64 is 2MB, the message size needed for the DiSCo-SLAM method for each LiDAR keyframe is around 200kB for VLP-16 while transmitting the keyframe feature cloud. On the contrary, in DCL-SLAM, the size of the LiDAR-Iris descriptors of each frame is 29.12kB, with sending filtered raw point cloud for verification (99.92kB/frame for VLP-16) in the loop closure message if necessary. The inter-robot match messages are mainly the loop measurement and verification laser point cloud. The last distributed PGO message mainly includes optimization states, the rotation, and pose estimates from the neighbor. In summary, our proposed DCL-SLAM will significantly reduce the communication burden without sharing raw data.

## V. CONCLUSIONS

This letter proposes a fully-distributed collaborative Li-DAR SLAM framework, namely DCL-SLAM, to complete a collaborative mapping task in an unknown environment with a robotic swarm. The proposed system is divided into three sub-modules: a flexible single-robot front-end, robust distributed loop closure, and distributed back-end with minimal information exchange. Experimental results on public and our campus datasets show the precision, rubostness, and broad applicability of our framework. In future work, we plan to explore the robustness of inter-loop closure modules, for example, adding more correlated outliers, and extend the framework to be compatible with solid-state LiDAR with more tests.

#### REFERENCES

- C. Cadena, L. Carlone, H. Carrillo, Y. Latif, D. Scaramuzza, J. Neira, I. Reid, and J. J. Leonard, "Past, present, and future of simultaneous localization and mapping: Toward the robust-perception age," *IEEE Transactions on robotics*, vol. 32, no. 6, pp. 1309–1332, 2016.
- [2] T. Shan, B. Englot, D. Meyers, W. Wang, C. Ratti, and D. Rus, "Lio-sam: Tightly-coupled lidar inertial odometry via smoothing and mapping," in 2020 IEEE/RSJ international conference on intelligent robots and systems (IROS). IEEE, 2020, pp. 5135–5142.
- [3] W. Xu, Y. Cai, D. He, J. Lin, and F. Zhang, "Fast-lio2: Fast direct lidar-inertial odometry," *IEEE Transactions on Robotics*, 2022.
- [4] P.-Y. Lajoie, B. Ramtoula, F. Wu, and G. Beltrame, "Towards collaborative simultaneous localization and mapping: a survey of the current research landscape," arXiv preprint arXiv:2108.08325, 2021.
- [5] K. Ebadi et al., "Lamp: Large-scale autonomous mapping and positioning for exploration of perceptually-degraded subterranean environments," in 2020 IEEE International Conference on Robotics and Automation (ICRA). IEEE, 2020, pp. 80–86.
- [6] Y. Chang et al., "Lamp 2.0: A robust multi-robot slam system for operation in challenging large-scale underground environments," ArXiv, vol. abs/2205.13135, 2022.

- [7] R. Dube, A. Cramariuc, D. Dugas, H. Sommer, M. Dymczyk, J. Nieto, R. Siegwart, and C. Cadena, "Segmap: Segment-based mapping and localization using data-driven descriptors," *The International Journal* of Robotics Research, vol. 39, no. 2-3, pp. 339–355, 2020.
- [8] Y. Huang, T. Shan, F. Chen, and B. Englot, "Disco-slam: Distributed scan context-enabled multi-robot lidar slam with two-stage globallocal graph optimization," *IEEE Robotics and Automation Letters*, vol. 7, no. 2, pp. 1150–1157, 2021.
- [9] Y. Wang, Z. Sun, C.-Z. Xu, S. E. Sarma, J. Yang, and H. Kong, "Lidar iris for loop-closure detection," in 2020 IEEE/RSJ International Conference on Intelligent Robots and Systems (IROS). IEEE, 2020, pp. 5769–5775.
- [10] J. G. Mangelson, D. Dominic, R. M. Eustice, and R. Vasudevan, "Pairwise consistent measurement set maximization for robust multi-robot map merging," in 2018 IEEE international conference on robotics and automation (ICRA). IEEE, 2018, pp. 2916–2923.
- [11] S. Choudhary, L. Carlone, C. Nieto, J. Rogers, H. I. Christensen, and F. Dellaert, "Distributed trajectory estimation with privacy and communication constraints: a two-stage distributed gauss-seidel approach," in *IEEE International Conference on Robotics and Automation* 2016, 2016.
- [12] R. Dubé, A. Gawel, H. Sommer, J. Nieto, R. Siegwart, and C. Cadena, "An online multi-robot slam system for 3d lidars," in 2017 IEEE/RSJ International Conference on Intelligent Robots and Systems (IROS), 2017, pp. 1004–1011.
- [13] P. Schmuck and M. Chli, "Ccm-slam: Robust and efficient centralized collaborative monocular simultaneous localization and mapping for robotic teams," *Journal of Field Robotics*, vol. 36, no. 4, pp. 763–781, 2019.
- [14] M. Karrer, P. Schmuck, and M. Chli, "Cvi-slam-collaborative visual-inertial slam," *IEEE Robotics and Automation Letters*, vol. 3, no. 4, pp. 2762–2769, 2018.
- [15] P. Schmuck, T. Ziegler, M. Karrer, J. Perraudin, and M. Chli, "Covins: Visual-inertial slam for centralized collaboration," in 2021 IEEE International Symposium on Mixed and Augmented Reality Adjunct (ISMAR-Adjunct). IEEE, 2021, pp. 171–176.
- [16] A. Cunningham, V. Indelman, and F. Dellaert, "Ddf-sam 2.0: Consistent distributed smoothing and mapping," in 2013 IEEE international conference on robotics and automation. IEEE, 2013, pp. 5220–5227.
- [17] T. Cieslewski, S. Choudhary, and D. Scaramuzza, "Data-efficient decentralized visual slam," in 2018 IEEE international conference on robotics and automation (ICRA). IEEE, 2018, pp. 2466–2473.
- [18] S. Choudhary, L. Carlone, C. Nieto, J. Rogers, H. I. Christensen, and F. Dellaert, "Distributed mapping with privacy and communication constraints: Lightweight algorithms and object-based models," *The International Journal of Robotics Research*, vol. 36, no. 12, pp. 1286– 1311, 2017.
- [19] H. A. Daoud, A. Q. Md. Sabri, C. K. Loo, and A. M. Mansoor, "Slamm: Visual monocular slam with continuous mapping using multiple maps," *PloS one*, vol. 13, no. 4, p. e0195878, 2018.
- [20] P.-Y. Lajoie, B. Ramtoula, Y. Chang, L. Carlone, and G. Beltrame, "Door-slam: Distributed, online, and outlier resilient slam for robotic teams," *IEEE Robotics and Automation Letters*, vol. 5, no. 2, pp. 1656– 1663, 2020.
- [21] Y. Chang, Y. Tian, J. P. How, and L. Carlone, "Kimera-multi: a system for distributed multi-robot metric-semantic simultaneous localization and mapping," in 2021 IEEE International Conference on Robotics and Automation (ICRA). IEEE, 2021, pp. 11210–11218.
- [22] Z.-C. Marton, D. Pangercic, R. B. Rusu, A. Holzbach, and M. Beetz, "Hierarchical object geometric categorization and appearance classification for mobile manipulation," in 2010 10th IEEE-RAS International Conference on Humanoid Robots. IEEE, 2010, pp. 365–370.
- [23] L. He, X. Wang, and H. Zhang, "M2dp: A novel 3d point cloud descriptor and its application in loop closure detection," in 2016 IEEE/RSJ International Conference on Intelligent Robots and Systems (IROS). IEEE, 2016, pp. 231–237.
- [24] G. Kim and A. Kim, "Scan context: Egocentric spatial descriptor for place recognition within 3d point cloud map," in 2018 IEEE/RSJ International Conference on Intelligent Robots and Systems (IROS). IEEE, 2018, pp. 4802–4809.
- [25] K. P. Cop, P. V. Borges, and R. Dubé, "Delight: An efficient descriptor for global localisation using lidar intensities," in 2018 IEEE International Conference on Robotics and Automation (ICRA). IEEE, 2018, pp. 3653–3660.

- [26] J. Zhang and S. Singh, "Loam: Lidar odometry and mapping in real-time." in *Robotics: Science and Systems*, vol. 2, no. 9. Berkeley, CA,
- time. In Robotics: Science and Systems, vol. 2, no. 9. Berkeley, CA, 2014, pp. 1–9.
  [27] K. Li, M. Li, and U. D. Hanebeck, "Towards high-performance solid-state-lidar-inertial odometry and mapping," *IEEE Robotics and Automation Letters*, vol. 6, no. 3, pp. 5167–5174, 2021.
  [28] M. Grupp, "evo: Python package for the evaluation of odometry and slam." https://github.com/MichaelGrupp/evo, 2017.